Osteoarthritis and Cartilage

OARSI OSTEOARTHRITIS RESEARCH SOCIETY INTERNATIONAL

Chondrocyte apoptosis in temporomandibular joint osteoarthritis promotes bone resorption by enhancing chemotaxis of osteoclast precursors

Y.N. Guo [†‡§], S.J. Cui [†‡§], Y.J. Tian [†‡§], N.R. Zhao [†‡§], Y.D. Zhang [†‡§], Y.H. Gan [†‡§ǁ¶], Y.H. Zhou [†‡§], X.D. Wang [†‡§]*

† Department of Orthodontics, Peking University School and Hospital of Stomatology, Beijing, China
‡ National Clinical Research Center for Oral Diseases & National Engineering Laboratory for Digital and Material Technology of Stomatology, Beijing, China
§ Beijing Key Laboratory of Digital Stomatology, 22# Zhongguancun South Avenue, Haidian District, Beijing, 100081, China
ǁ Center for Temporomandibular Disorders and Orofacial Pain, Peking University School and Hospital of Stomatology, Haidian District, Beijing, China
¶ Central Laboratory, Peking University School and Hospital of Stomatology, Haidian District, Beijing, China

ARTICLE INFO

SUMMARY

Objective: This study aimed to explore the effect and mechanism of chondrocyte apoptosis on the chemotaxis of osteoclast precursors (OCPs) during bone destruction.
Design: The relationship between cartilage and bone destruction was verified with a rat temporomandibular joint osteoarthritis (TMJOA) model. The pan-caspase inhibitor Z-VAD-FMK (ZVAD) was applied to confirm the chemotactic effect of chondrocyte apoptosis on OCPs. Synthesis and release of the key chemokine CX3CL1 in apoptotic and non-apoptotic chondrocytes was assessed with IHC, IF, WB, and ELISA. The function of CX3CL1-CX3CR1 axis in the chemotaxis of OCPs was examined by CX3XR1 inhibitor AZD8797 (AZD) and si-CX3CL1. The regulatory effect of p38 MAPK on CX3CL1 release was verified by p38 inhibitor PH-797804.
Results: A temporal and spatial association between cartilage degradation and bone resorption was found in the TMJOA model. The caspase-dependent chondrocyte apoptosis promoted chemotaxis of OCPs, which can be restrained by ZVAD. CX3CL1 was significantly upregulated when chondrocytes underwent apoptosis, and it played a critical role in the recruitment of OCPs, blockage of CX3CL1-CX3CR1 axis resulted in less bone resorption in TMJOA. P38 MAPK was activated in apoptotic chondrocytes, and had a regulatory effect on the synthesis and release of CX3CL1. After inhibition of p38 by PH-797804, the chemotactic effect of apoptotic chondrocytes on OCPs was limited.
Conclusions: This study indicates that apoptosis of chondrocytes in TMJOA enhances chemotaxis of OCPs toward osteoclast precursors through upregulation of the p38-CX3CL1 axis, thereby promoting the activation of local osteoclasts.

Introduction

Temporomandibular joint osteoarthritis (TMJOA) is the major type of degenerateive joint disease (DJD) of temporomandibular joints (TMJ), and a serious subtype of temporomandibular disorders (TMD) which leads to chronic pain and dysfunction of mandibular movements.

Traditional treatments for TMJOA include non-surgical and surgical options. Non-surgical treatments include non-steroidal anti-inflammatory drugs (NSAIDs) therapy[1], physical therapy[2], occlusal pad therapy[3,4], and arthrocentesis[5]. Although commonly used, NSAIDs have been shown to be involved in a variety of drug interactions, as determined by different artificial intelligence methods that assess ER data[6]. Surgical interventions, such as joint replacement with autologous bone or artificial joints, are only used in severe cases of impaired joint function, significant degenerative disease, and intractable pain[7].

Although these therapies can relieve pain and restore joint function to some extent, better treatment options are needed, supporting the need for further exploration of TMJOA pathogenesis
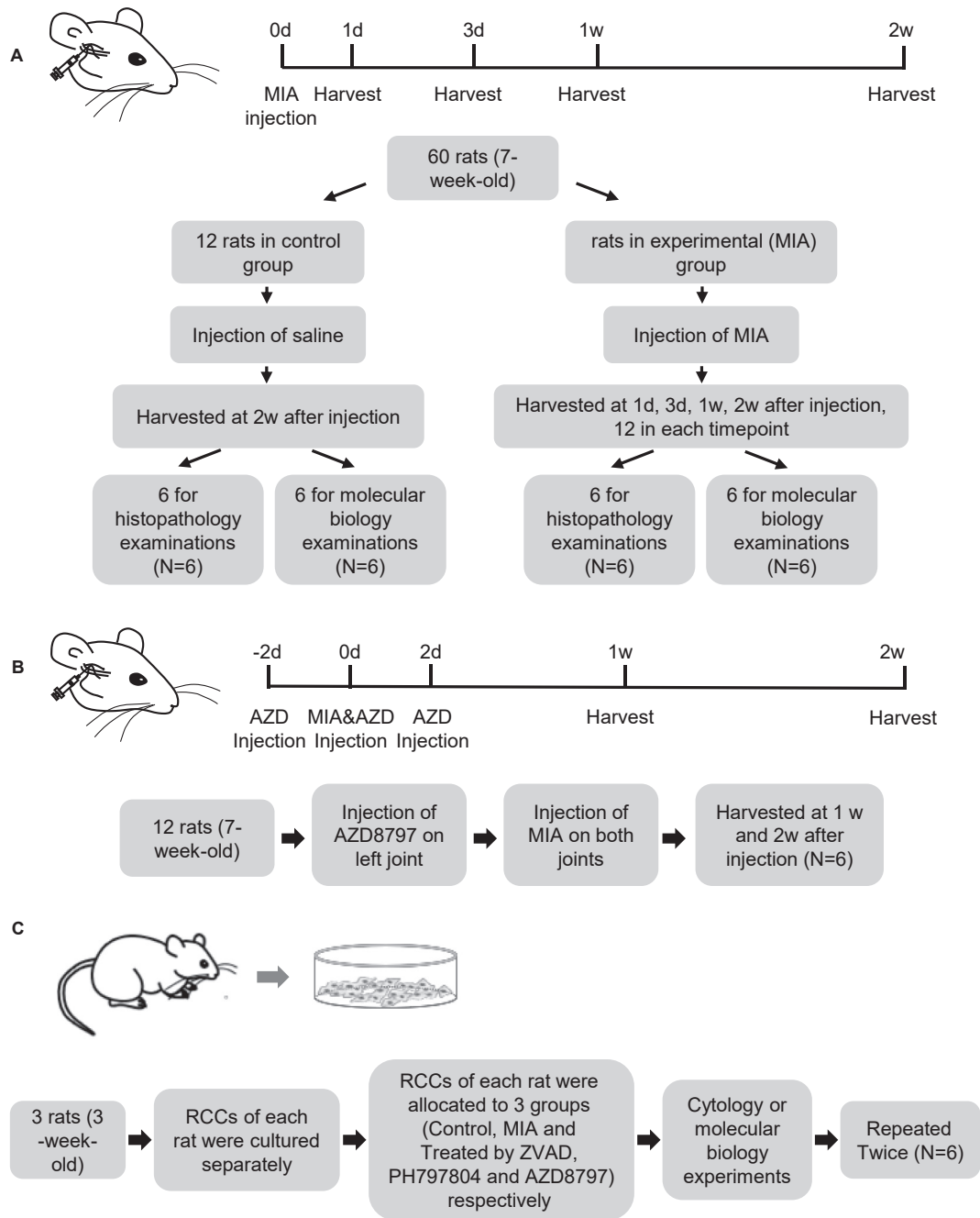
* Address correspondence and reprint requests to: X.D. Wang, Department of Orthodontics, Peking University School and Hospital of Stomatology, 22# Zhongguancun South Avenue, Beijing, 100081, China. Tel.: 86 10 82195332; Fax: 86 10 82195336.

*E-mail address:* wangxuedong@bjmu.edu.cn (X.D. Wang).

Fig. 1

Outline of experimental design. TMJOA model induced by injection of 0.5 mg monosodium iodoacetate (MIA). (A) The experimental schedule and allocation of animals in the observational experiment; the TMJs were harvested 1 day, 3 days, 1 week, and 2 weeks after injection. (B) The experimental schedule and allocation of animals in the therapeutic experiment; the AZD8797 (AZD) was injected 2 days before, 0 day, and 2 days after MIA injection. (C) The cytology and molecular biology experiments were conducted on rat condylar chondrocytes (RCCs) from at least six different sources and each cell culture was divided into three groups: Control, MIA, and MIA with inhibitor.
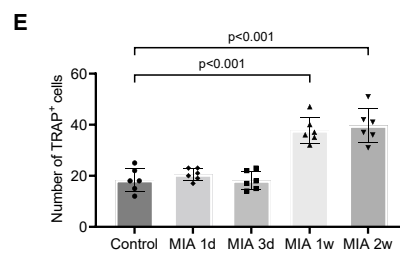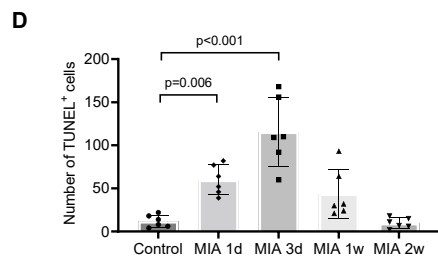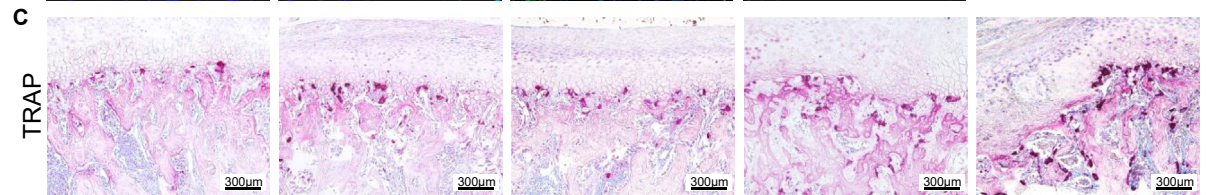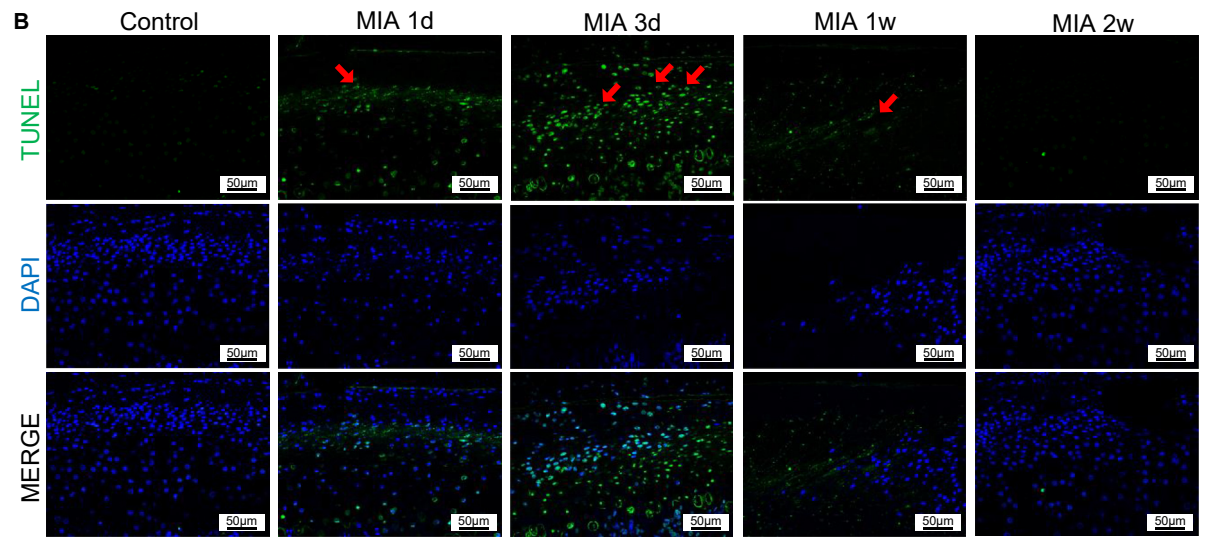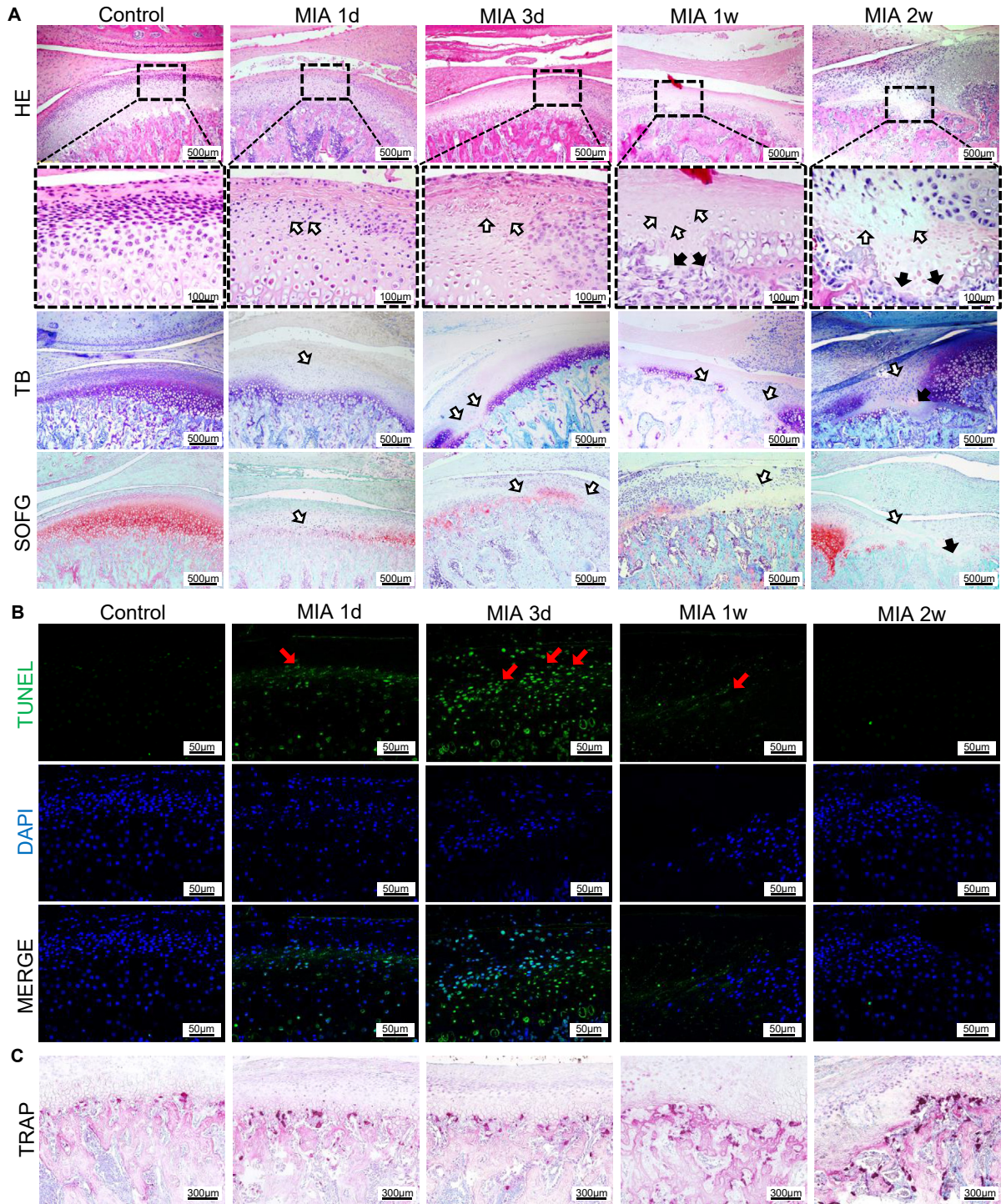
to determine novel disease targets and mechanisms can be therapeutically targeted.

Clinical pathological analysis of TMJOA involves discontinuity of the cartilage matrix and clusters of hypertrophic or dead chondrocytes, with increased resorption and lacunae in the subchondral bone[8]. Spatial correlation of cartilage degradation and bone resorption (the two leading pathological characteristics of TMJOA) is not fully understood, but reports have indicated a potential relationship between these two pathological processes[9–11]. At present, there are two views.

The first states that bone destruction initiates TMJOA, because subchondral bone lesions can be observed before cartilage damage by MRI[12]. Meanwhile, overexpression of transforming growth factor β (TGF-β) in subchondral bone contributes to cartilage degradation in TMJOA[13].

The second view is that cartilage destruction occurs before bone destruction, and degraded cartilage releases a variety of cytokines, like nuclear factor-κ B ligand (RANKL), stromal cell-derived factor 1 (SDF-1), and TGF-β1, which all promote local osteoclast activation[14,15]. In addition, degeneration of cartilage can alter local mechanical loading properties, causing more damage to the underlying bone[16].

Generally speaking, the mutual effect of cartilage and bone damage can reinforce each other in the progression of OA, but the mechanism behind this is not certain. Focusing on the cellular level, the hypocellular cartilage caused by chondrocyte apoptosis is closely related to osteoarthritis[17,18]. In various TMJOA models, chondrocyte apoptosis was found to be significantly enhanced[19–22]. As for bone resorption, the osteoclast is the main effector cell, and is activated by the compound result of the recruitment and differentiation of osteoclast precursor (OCP) represented by bone marrow-derived macrophages/monocytes (BMMs). Whether chondrocyte apoptosis has a direct influence on the activation process remains unclear.

In our previous studies, we created a typical TMJOA model by intra-articular injection of monosodium iodoacetate (MIA), which induced a progression of cartilage degradation, bone resorption, and pain. Interestingly, time-course tissue section staining showed a sequence of chondrocyte apoptosis and activation of local osteoclasts[20,23]. Therefore, this model is appropriate for exploring the influence of chondrocyte apoptosis on osteoclast activation. In turn, this could reveal the interaction of different tissues in a novel way, and may provide an effective strategy for the treatment of TMJOA.

Materials and methods

Induction of TMJOA

The animal model was established according to our previous studies[20]. Healthy Sprague-Dawley rats (200 ± 20 g, 7 weeks old) were obtained from SPF Experimental Animal Co., Ltd. (Beijing, China). In order to manipulate the clinical high female-to male preponderance[23], only female rats were examined.

In the observational experiment, 60 rats were randomly assigned to two groups: experimental (n = 48) and control (n = 12). Following i.p. anesthetic injection of pentobarbital, TMJOA was induced in the experimental group by injection of 0.5 mg MIA (Sigma, Saint Louis, USA) dissolved in 50 μL saline into the upper compartment of bilateral TMJs using a 27-gauge/0.5-inch needle without surgical assistance. The control group received bilateral injection with 50 μL saline only. The experimental group was sacrificed at 1 day, 3 days, 1 week, and 2 weeks after MIA injection, with 12 rats at each timepoint. The control group was sacrificed 2 weeks after saline injection (Fig. 1(A).).

In the therapeutic experiment, both TMJs of 12 rats received MIA injection as described above. In addition, their left TMJ was injected with 125 μg AZD8797 (AZD, MedChemExpress, USA), which was dissolved in 50 μL solvent containing 10% DMSO, 40% PEG300, 5% Tween-80, and 45% saline as recommended by the manufacturer, at 2 days before MIA injection, the day of MIA injection, and 2 days after MIA injection. The right TMJ was injected with the solvent at the same timepoints. The rats were sacrifice at 1 week and 2 weeks after MIA injection, with six rats at each timepoint (Fig. 1(B).).

All animal procedures were approved by the Peking University Animal Ethics Committee prior to the initiation of the study (Approval number: LA2014221). The methods employed were performed in accordance with approved guidelines.

Tissue harvesting

The rats were sacrificed as scheduled by injection of pentobarbital.

In the observational experiment, the unilateral TMJs of six rats at each time point were used for histopathological examination and the unilateral TMJs from the other six rats were used for molecular biology experiments. For histopathological examination, TMJs were carefully removed en bloc, fixed in 4% paraformaldehyde for 24 h, and then demineralized in 15% EDTA. For molecular biology experiments, only the condyle apex was dissected and used for later examinations.

In the therapeutic experiment, all TMJs were fixed in 4% paraformaldehyde for 24 h and received micro CT scanning, then they were demineralized in 15% EDTA.

Histopathologic staining

TMJ blocs were paraffin-embedded and cut in serial sagittal sections of 5 μm. For morphological evaluation, the sections were stained with hematoxylin and eosin (HE). Toluidine blue (TB)

Fig. 2 | Osteoarthritis and Cartilage

Cartilage degradation and bone resorption were spatially correlated in the TMJOA model. To observe the feature of TMJOA, TMJs in different groups were sectioned in sagittal for HE, TB, SOFG, TUNEL, and TRAP staining. (A) HE, TB and SOFG staining showing the time-dependent changes of the condyle in the TMJOA model induced by MIA injection (0.5 mg/joint; 1 day to 2 weeks), cartilage degradation and bone resorption are shown by white and black arrows respectively. (B) TUNEL staining showing the apoptotic chondrocytes in condylar cartilage, which were marked by red arrows. (C) TRAP staining showing the increased activity of osteoclast after injection. (D) and (E) Quantification of the number of positive cells in each view. Data are presented by mean ± SD (n = 6). Statistical significance was assessed by one-way ANOVA for comparisons between multiple groups, and **P**-values were calculated by Dunnett's test for multiple comparisons between the control group and other groups.
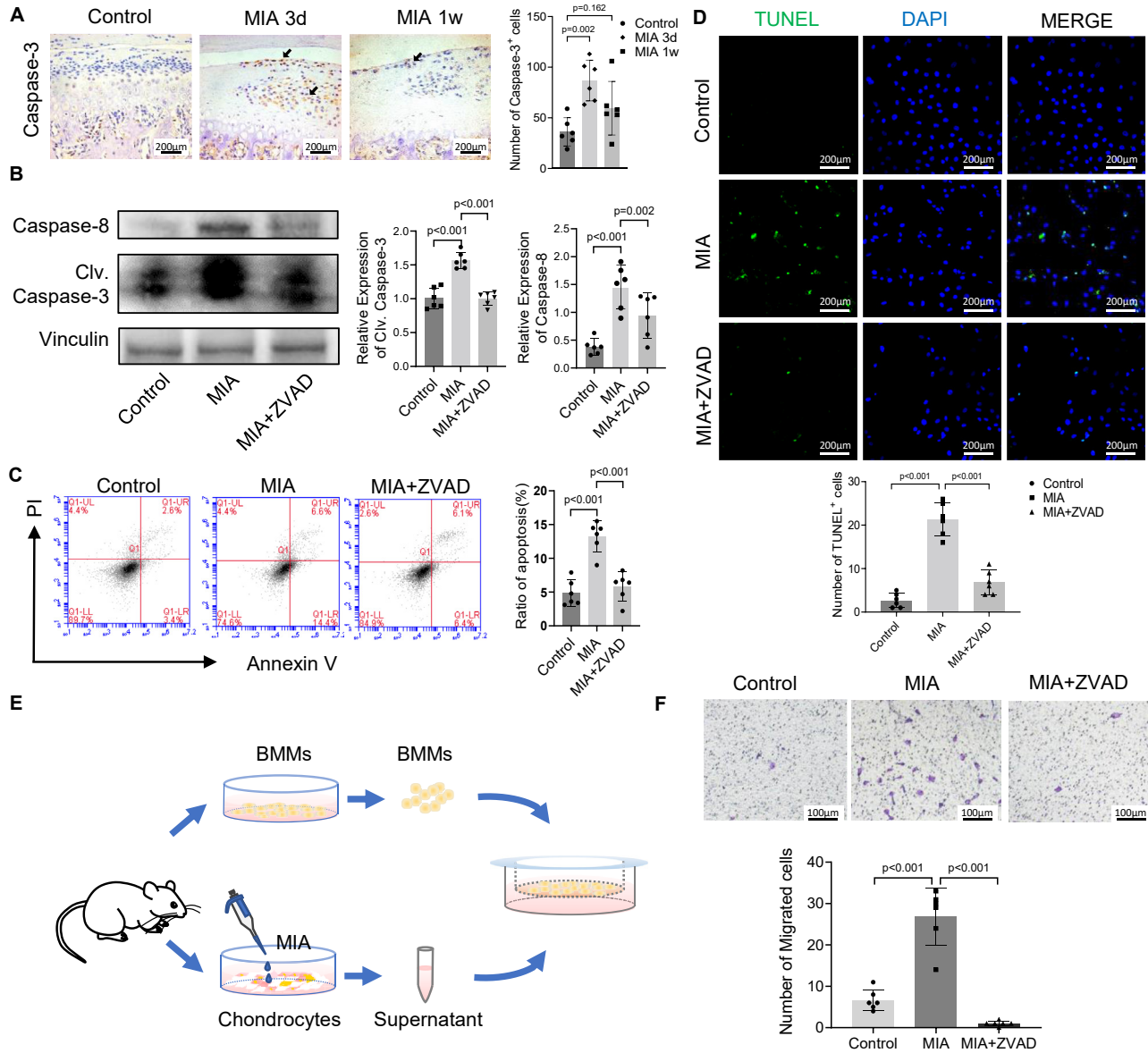
Fig. 3

Osteoarthritis and Cartilage

MIA induced apoptosis and enhanced chemotactic effect in TMJ chondrocytes. (A) Immunohistochemical (IHC) staining and quantification of caspase-3 positive cells in the condylar cartilage of rats induced by MIA injection. (B) Protein expression of caspase-family *in vitro*, data represented are mean fold change normalized to Vinculin. (C) Flow cytometry was applied to evaluate the apoptosis of TMJ chondrocytes using a FITC-annexin V/PI apoptosis analysis assay kit. (D) TUNEL staining showing the apoptosis cells with green fluorescence. (E) Schematic diagram of the *in vitro* migration assay. (F) Migration of BMMs promoted by the supernatant of apoptotic chondrocytes, quantified by the number of migrated cells in each view. Data are presented by mean ± SD (n = 6). One-way ANOVA was used to evaluate the significance between multiple groups in (A), and Dunnett test was used to calculate the *P*-value for post-hoc comparisons. Two-way ANOVA was used to evaluate the significance between multiple groups in (B, C, D, F), and the Tukey test was used to calculate the *P*-value for post-hoc comparisons.

stains and safranin-O and fast green (SOFG) stains were performed by TB kit and SOFG kit (Solarbio, China) to show the degree of cartilage degradation. Tartrate-resistant acid phosphatase (TRAP) stains were performed by a TRAP/ALP stain kit (Wako Pure Chemical Industries, Japan) in order to evaluate the activation of local osteoclast. For TRAP staining, sections of left TMJs from six different rats were selected and counted by three experienced researchers who were blinded to the groups. The number of positive cells in three randomly selected views were recorded and averaged.

Culture of rat condylar chondrocytes (RCCs)

Primary chondrocytes were obtained from TMJs of three-week-old female rats, cells from different rats were cultured separately. Rat condylar chondrocytes (RCCs) from at least six rats were tested in every experiment. The cartilage layer of the condyle was dissected carefully and digested with 0.25% trypsin (Hyclone, USA) for 10 min, followed by 0.25% type II collagenase (Sigma-Aldrich, USA) for 1.5 h. The chondrocytes were then resuspended and cultured in Dulbecco's modified Eagle's medium (DMEM, Hyclone) containing 10% fetal bovine serum (FBS; Gibco) under 5% CO_2 at 37°C. RCCs were used for experiments in two passages. As illustrated in Fig. 1(C), every cell culture was divided into three groups as follows: the control group was cultured without any stimulation; the MIA group was stimulated by 5 μM MIA for 24 h; and the treated group was pretreated by different inhibitors 1 h in advance of MIA stimulation. The following inhibitors were applied in this study: 10 μM Z-VAD-FMK (ZVAD, MedChemExpress, USA), 2 μM AZD8797 (AZD, MedChemExpress, USA), 2 μM PH-797804 (MedChemExpress, USA).

Quantitative analysis of apoptotic cells

RCCs (described above) were randomly divided into three groups: control group, MIA group and MIA + ZVAD group. Flow cytometry was used to quantify the changes of cell apoptosis by loading FITC-annexin V/PI double-fluorescence labeling. Collected chondrocytes were labelled by Annexin V-FITC Apoptosis Detection Kit (Solarbio, China) as instructed, then measured by flow cytometry (BD Accuri C6 Plus, New Jersey, USA). Data were analyzed using CFlow Plus software.

In vitro migration assay

The culture medium of RCCs in different groups (e.g., control group, MIA group and MIA + ZVAD group) were collected and centrifugated at 1,000×g, each group contained at least six samples from different cell cultures. The supernatant was collected and placed into the lower chamber of a 24-well Transwell insert (3 μm, Corning Life Sciences, USA). Each chamber contained 600 μL supernatant. Next, 1×10^5 BMMs were collected and resuspended at 100 μL α-MEM containing 10% FBS, then seeded onto the upper chamber of the Transwell insert. After co-culturing for 12 h, cells remaining on the top of the Transwell membrane were gently removed and discarded, and the membrane was fixed with 4% paraformaldehyde, and stained with crystal violet for 30 min. The membrane was observed and photographed by microscope. The number of migrated BMMs from six randomly selected fields was counted under microscope by three blinded researchers, and the means were used for statistical analysis.

The following methods are described in detail in the Appendix:

- Micro CT examination
- Immunohistochemistry staining
- Confocal Imaging
- Terminal Deoxynucleotidyl Transferase dUTP nick-end Labeling (TUNEL) Assay
- Culture of rat BMMs
- siRNAs and cell transfection
- Real-time polymerase chain reaction
- Western blot analysis
- Enzyme-linked immunosorbent assay

Statistical analysis

Statistical analysis and graphing were performed using GraphPad Prism v9.3. All samples were included in the analysis unless reliable result was unable to obtain because of the decomposition or contamination, and data was presented as mean ± SD. For the observational experiment *in vivo*, one-way ANOVA was used for comparisons across multiple groups, and Dunnett's test was used for post-hoc multiple comparisons. Paired *t*-test was used in the therapeutic experiment. For the *in vitro* experiments, two-way ANOVA was used for comparisons across multiple groups, and Tukey's test was used for *post-hoc* multiple comparisons. A *P* value < 0.05 was considered statistically significant.

Results

Temporal and spatial relationships between chondrocyte apoptosis and subchondral bone destruction in the early stage of TMJOA

An observational experiment was conducted in order to manifest the feature of TMJOA, and the histopathology change in different groups were evaluated. In control group, superimposed chondrocytes were laid regularly in a thick cartilage layer as far as the area of transition with the bone tissue. In the subchondral bone area, the trabecula was even and continuous, and the shape was complete. A typical TMJOA-like change was observed in the MIA group, which first manifested as shrunken and broken chondrocytes in the condylar cartilage. Three days after injection, nuclear condensation, cell loss, and less matrix staining of the cartilage layer appeared mostly in the middle zone within the sections. One week after injection, matrix loss expanded to the whole cartilage layer, and bone destruction occurred just below the cartilage damage. After another week, the deformity became more significant, in that both cartilage and bone lost normal morphology [Fig. 2(A)].

To demonstrate apoptosis in the chondrocytes, we developed a Transferase dUTP nick-end Labeling (TUNEL) staining to illuminate broken DNA. Fluorescence observation showed a significant increase of apoptotic cells in the experimental group, which peaked at 3 days after MIA injection [Fig. 2(B) and (D)]. Also, TRAP staining showed a progressing increase of osteoclasts and an enhance of osteoclast (OC) activity just below the cartilage destruction, where bone destruction occurred [Fig. 2(C) and (E)].

Chondrocyte apoptosis is driven by caspase family

The caspase family was significantly activated in the TMJOA model (Fig. 3). Classic apoptosis was characterized by the cascades of caspase family members, and caspase-3 is the main executor in this process. IHC staining showed a significant increase of caspase-3 positive cells in the MIA injected group [Fig. 3(A)]. In the sections 3 days after MIA injection, an apparent increase of caspase-3 positive cells was observed in whole layers of cartilage near the destructed area.

An *in vitro* model also showed typical apoptosis in chondrocytes. After a 24-h stimulation of MIA, caspase-8 and caspase-3 were up-regulated significantly, implying that apoptosis was mediated by the caspase family. To confirm the critical role of caspase cascades in this model, Z-VAD-FMK (ZVAD), a pan-caspase inhibitor, was added into the culture medium 1 h before the MIA stimulation. This decreased the expression of caspase family significantly [Fig. 3(B)]. Flow cytometry showed the positive rate of Annexin V (representing the early stage of apoptosis)
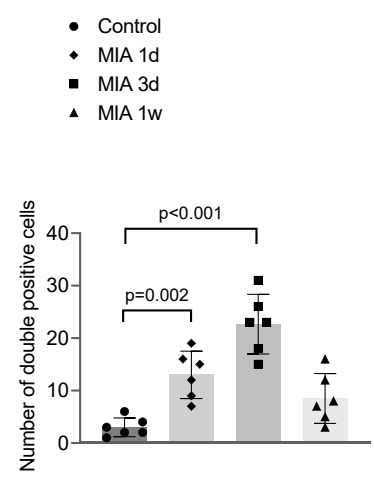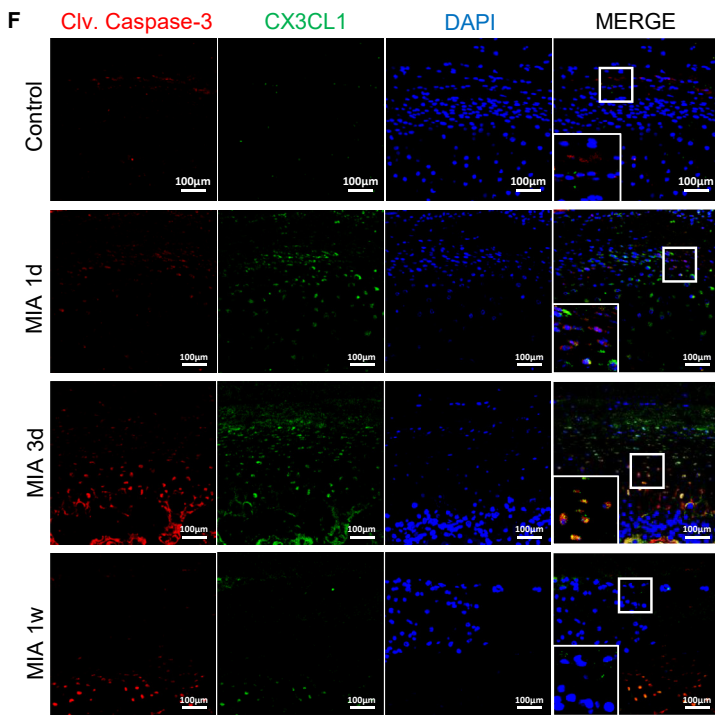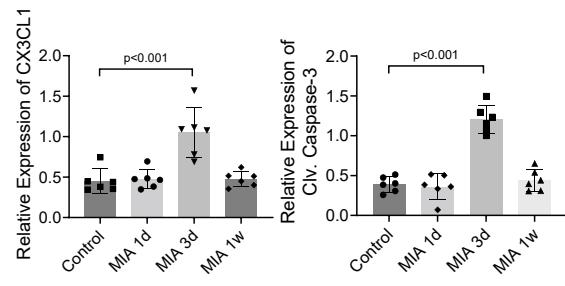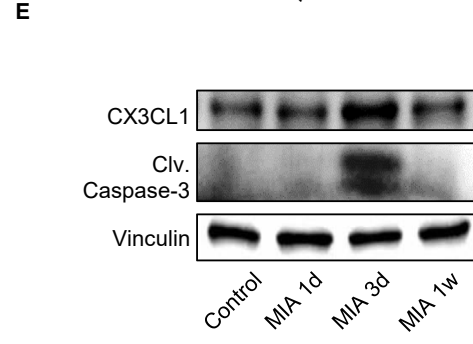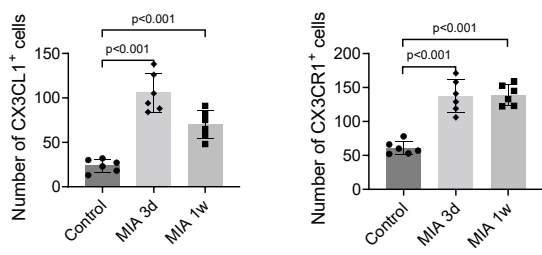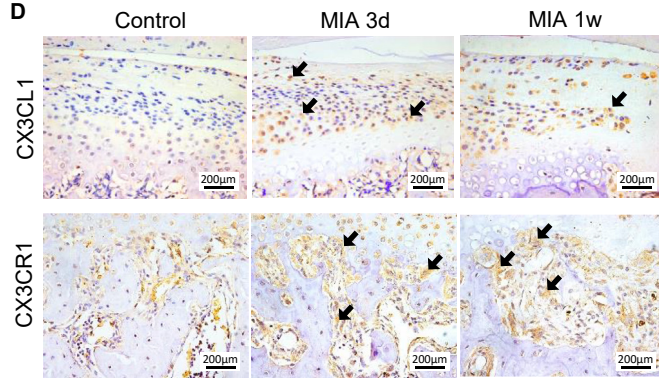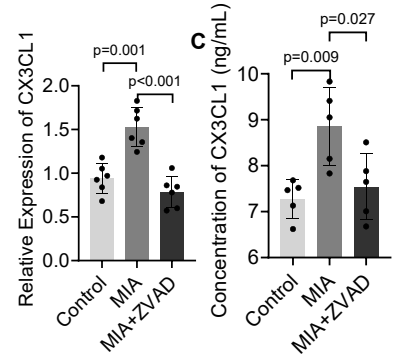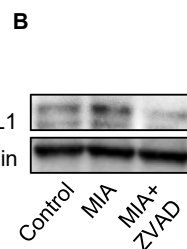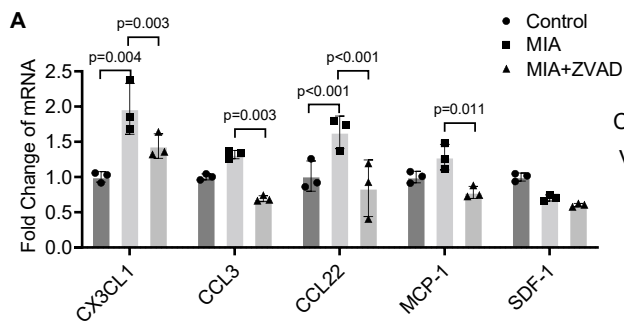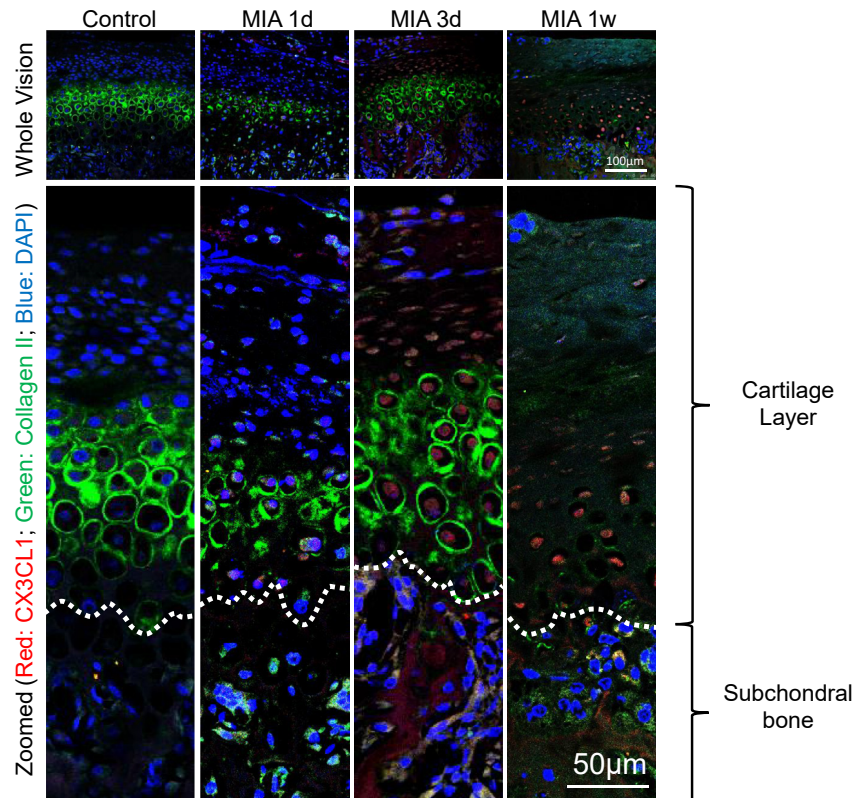
Fig. 5

CX3CL1 positive cells expanded into the subchondral bone area. Sectioned TMJs were stained to identify CX3CL1 (red) and collagen II (green), the white dotted line indicates the cartilage-bone interface.

increased significantly in MIA group and that rate dropped back when ZVAD was added [Fig. 3(C)]. In consistent with the flow cemetery results, TUNEL staining showed an increase of apoptotic cells in the MIA group, and a reduction in the MIA + ZVAD group [Fig. 3(D)].

Apoptosis environment of chondrocyte enhances the chemotaxis of BMMs

Previous studies showed that apoptotic cells can induce efferocytosis, which features the release of a set of molecules, the attraction of phagocytes, and the swift clearance of the dead apoptotic cells[24]. Originating from monocytes, osteoclast precursors (OCPs) also express certain chemokine receptors. We questioned whether OCPs can be attracted by the process of chondrocyte apoptosis, and if this is the reason of more OC activation in TMJOA models?

To evaluate the chemotaxis of BMMs, a Transwell experiment was conducted. Crystal violet staining showed that the culture medium of the MIA group can attract significantly more BMMs than either the culture medium of the control or the MIA + ZVAD group (Fig. 3(E) and (F)).

Fig. 4

Chemokine CX3CL1 was up-regulated by MIA stimulation. (A) Apoptotic environment of chondrocytes increased the expression of chemokines and was restrained by Z-VAD-FMK (ZVAD). (B) WB showing the expression of CX3CL1 in MIA and MIA + ZVAD group. (C) The release of CX3CL1 in the supernatant was evaluated by ELISA. (D) IHC staining and quantification of CX3CL1 positive cells in condylar cartilage and CX3CR1 positive cells in subchondral bone. Arrows indicate the positive cells. (E) Change of protein expression of CX3CL1 in condyle induced by MIA injection, data presented are mean fold change normalized to Vinculin (n = 6). (F) Sectioned TMJs were stained with cleaved (Clv.) Caspase 3 (red) and CX3CL1 (green). Quantified by the number of double-positive cells in each view, data are presented by mean ± SD. Two-way ANOVA was used to evaluate the significance between multiple groups in (A−C), and the Tukey test was used to calculate the *P*-value for post-hoc comparisons. One-way ANOVA was used to evaluate the significance between multiple groups in (D−F), and Dunnett test was used to calculate the *P*-value for post-hoc comparisons.
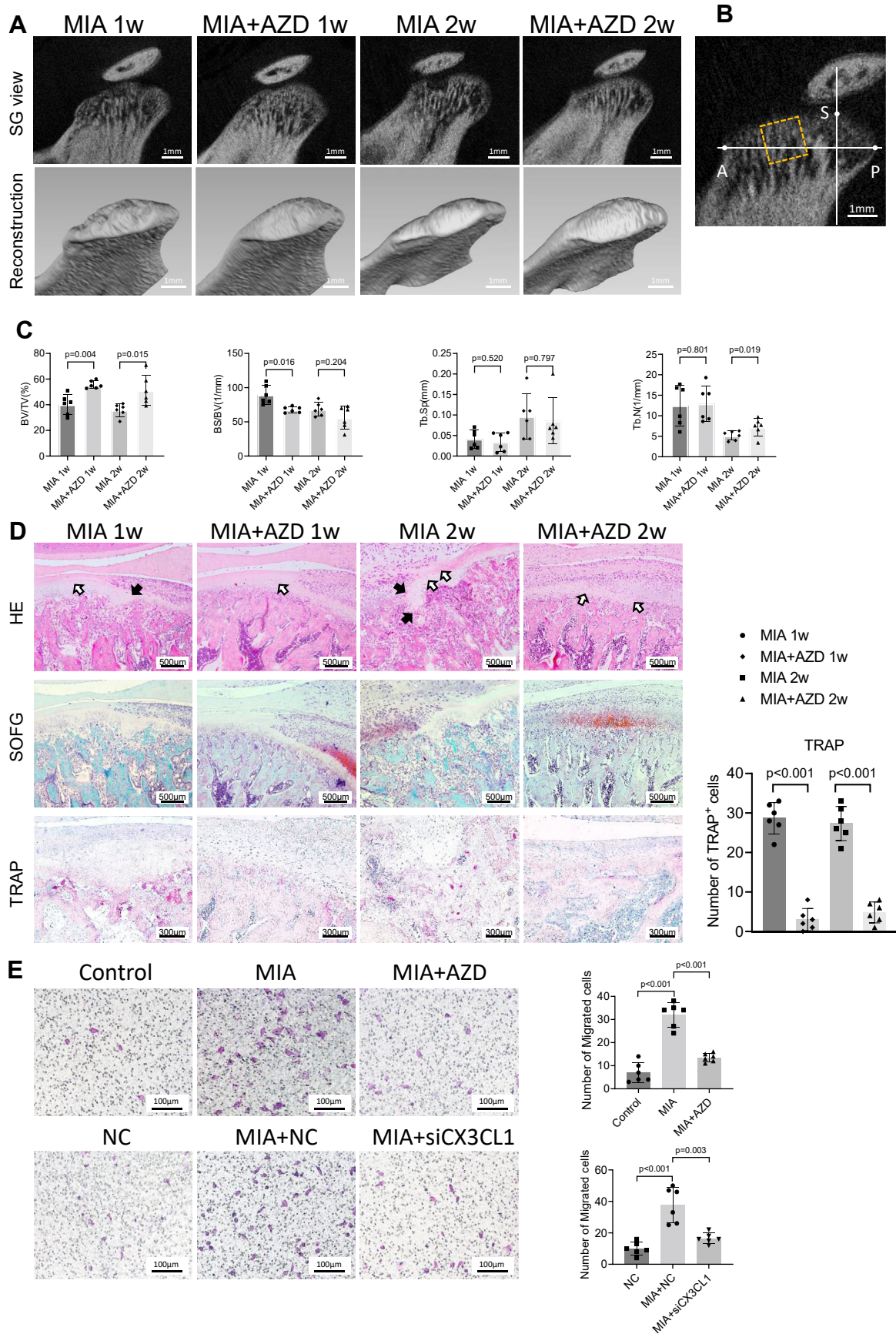
The apoptosis of chondrocyte promotes the release of CX3CL1

Gene expression analysis indicated that the chemokines were up-regulated in MIA group, and that this increase was restrained by the application of ZVAD [Fig. 4(A)]. Among the several common chemokines tested in the gene expression analysis, the C-X3-C motif chemokine ligand 1 (CX3CL1, also called fractalkine), which showed a remarkable change in MIA and MIA + ZVAD group, drew our attention. CX3CL1 is a membrane-bound chemokine and the only known member of the CX3C subfamily. Previous studies revealed its function as a "find-me" signal in cell apoptosis[25,26]. Unlike most chemokines, it has both a membrane-bound and soluble form, and a dual function of both attracting and adhering. Many immune cells are attracted by CX3CL1, including monocytes and NK cells. Koizumi *et al.* discovered that CX3CR1, the receptor of CX3CL1, is expressed by OCPs, but not mature osteoclasts[27]. Hoshino *et al.* confirmed that the CX3CL1-CX3CR1 axis plays a critical role in both the chemotaxis and maintenance of OCPs[28]. Many clinical studies have shown an increase of CX3CL1 in the synovial fluid of OA patients[29,30]. However, the origin of the increased CX3CL1 in OA patients is still unclear.

In vitro analysis showed that both the soluble form and the total amount of CX3CL1 increased significantly in MIA group, and decreased with the application of ZVAD (Fig. 4(B) and (C)). This demonstrates that the apoptosis environment plays a certain regulatory role in the expression of CX3CL1.

IHC staining confirmed the increase of CX3CL1 and its receptor, C-X3-C motif chemokine receptor 1 (CX3CR1), in the TMJOA model in both 3-day and 1-week after injection samples [Fig. 4(D)]. There, the number of CX3CL1 positive chondrocytes in fibrous layer and proliferative layer increased substantially. The number of CX3CR1 positive cell increased in the subchondral bone of MIA groups. WB of the condyle samples confirmed that the expressional change of CX3CL1 and cleaved caspase-3 were highly synchronous [Fig. 4(E)].

Immunofluorescent staining confirmed the spatial relationship between cleaved caspase-3 and CX3CL1 [Fig. 4(F)]. Condyle sections of control and TMJOA rats were doubled stained with cleaved caspase-3 (which marked the apoptotic cells with red) and CX3CL1 (marked with green). In the control group, few cleaved caspase-3 or CX3CL1 molecules were detected. In contrast, an increase in cleaved caspase-3 and CX3CL1 were observed as the TMJOA progressed, which peaked at 3 days after injection. In addition, a high degree of co-localization between cleaved caspase-3 and CX3CL1 was observed in the area of cartilage destruction.

Moreover, positive expression of CX3CL1 showed a downward trend during the transition from the superficial zone of cartilage to the subchondral bone. In Fig. 5, condyle sections were stained to identify CX3CL1 (marked with red) and collagen II (which marked cartilage, especially the calcified layer, with green). In the control

group, CX3CL1 expression was low. In sections 1 day after MIA injection, the highest expression of CX3CL1 was detected in the fibrous layer. In sections 3 days after MIA injection, the strongest expression of CX3CL1 moved into the calcified layer, and the subchondral bone area also showed obvious positive staining. One week after injection, positive staining began to weaken but was still detectable in both the calcified layer and the subchondral bone.

CX3CL1 enhances the chemotaxis of OCPs

To verify the relationship between CX3CL1 and the recruitment of OCPs, we applied AZD8797 (AZD), a CX3CR1 specified inhibitor, *in vivo* and *in vitro*. In our animal model, 12 rats were injected with MIA in both TMJs and then received a therapeutic dose of AZD8797 only in their left TMJs.

To evaluate bone destruction within the condyles, micro CT was applied to all the TMJs. The subchondral bone surface in the MIA group was discontinuous, as defined by decreased trabecular bone and regional bone defects 1 week after MIA injection. These deformities were increasingly obvious at 2 weeks after MIA injection. In the MIA + AZD group, however, the destruction was much milder, and the bone volume was higher [Fig. 6(A), (B), and (C)].

The difference seen between these two groups was supported by histopathologic staining [Fig. 6(D)]. Using HE and SOFG staining, condyles in the MIA group were shown to be severely damaged and deformed in subchondral bone. As for the MIA + AZD group, although cartilage degradation still occurred, the associated bone destruction was minor. TRAP staining also showed a significant suppression of osteoclast activation in the MIA + AZD group. The number of osteoclasts in the MIA group was much higher at both timepoints.

To determine the function of CX3CL1 *in vitro*, transwell experiments were conducted. We utilized two methods to block the CX3CL1-CX3CR1 axis: 1) knockdown of CX3CL1 expression by siRNA (50 nM, Ribobio, China) and 2) decreased CX3CR1 signaling by using CX3CR1 inhibitor AZD8797. The former was added into RCCs' culture medium 24 h before MIA stimulation. The latter was added at a concentration of 2 μM directly into the lower chamber in the transwell system. Both methods reduced the number of migrated BMMs significantly [Fig. 6(E)].

Activation of p38 MAPK is involved in the regulation of CX3CL1 released by apoptotic chondrocytes

Although the release of CX3CL1 is confirmed to be strongly related to apoptosis, the mechanism is not very clear. In order to determine which pathway plays a critical role in our model, WB was carried out to evaluate the change of key proteins in pathways that were found to be involved in the CX3CL1 release[31−36]. Among

Fig. 6   Osteoarthritis and Cartilage

Blocking CX3CL1-CX3CR1 axis attenuated bone destruction by reducing OCPs recruitment. AZD8797 was injected to the left joint of TMJOA rats as a therapeutic method in order to evaluate the function of CX3CL1-CX3CR1 axis. (A) Representative sagittal view and 3-dimensional reconstruction of samples harvested at 1 week and 2 weeks after MIA injection (B) Schematic diagram of volume of interest (VOI). A 1.3 mm × 1.3 mm × 0.3 mm region on the anterior inclined plane was selected to measure the bone-related parameters. The yellow box represents the cross section of VOI: A, most anterior position; P, most posterior position; S, most superficial position of condyle head. (C) Bone deterioration related parameters in the VOI of all samples. (D) HE, SOFG and TRAP staining showing the pathology feature of MIA and MIA + AZD group, cartilage degradation and bone resorption are marked by white and black arrows respectively. The activation of osteoclasts was quantified by the number of TRAP positive cells in each view. (E) The MIA-induced migration of BMMs canceled by knock-down of CX3CL1 and inhibition of CX3CR1, quantified by the number of migrated cells in each view. Data are presented by mean ± SD (n = 6). Paired *t*-test was used to evaluate the significance in (C, D). Two-way ANOVA was used to evaluate the significance between multiple groups in (E), and the Tukey test was used to calculate the **P**-value for *post-hoc* comparisons.
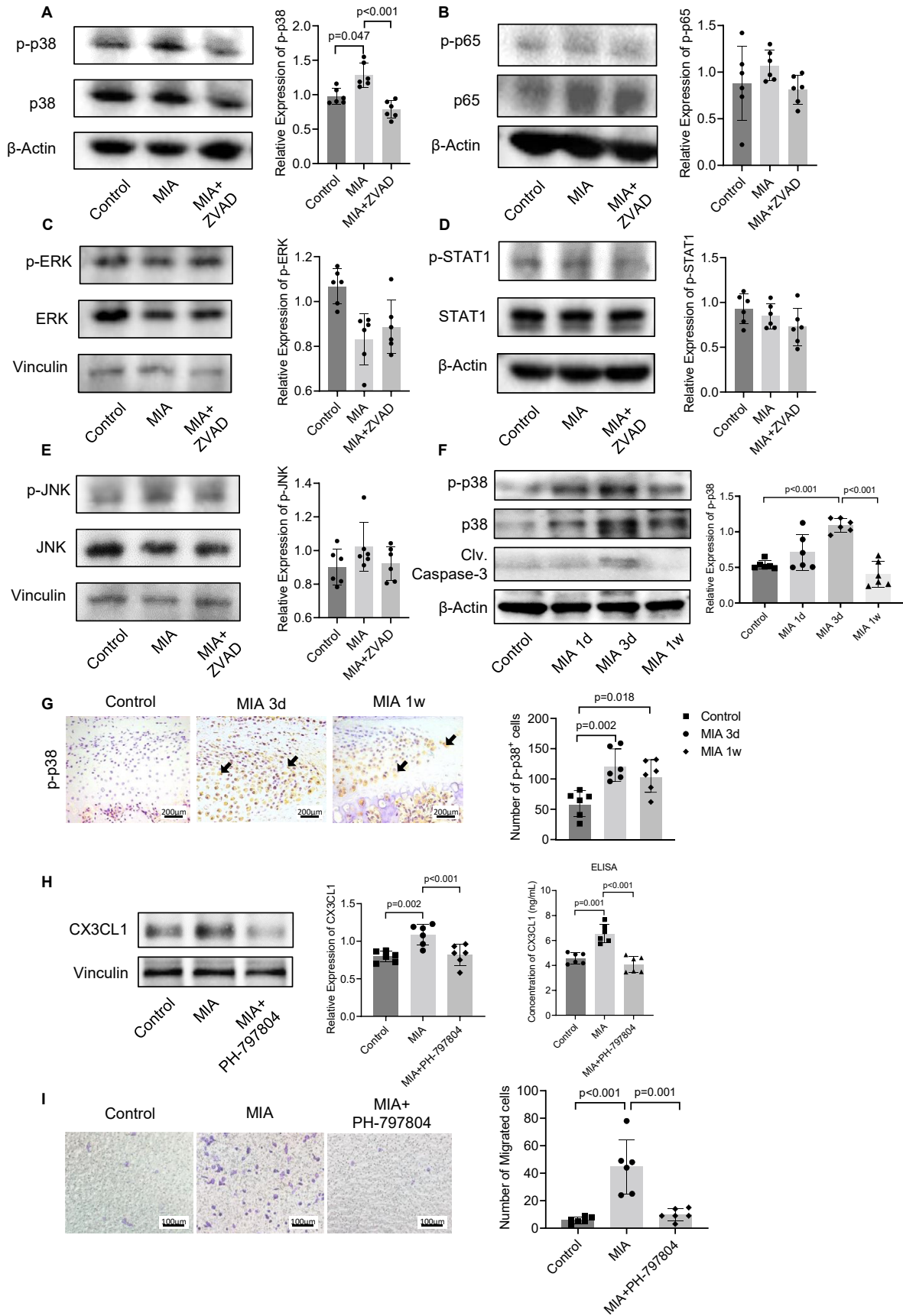
the possible pathways mentioned above, the phosphorylation of p38 MAPK showed the most significant change [Fig. 7(A)–(E)].

Interestingly, the promoted p38 MAPK in MIA group was also suppressed by ZVAD, indicating that the apoptosis environment is one of the initiating factors. *In vivo* WB showed that the expression of p-p38 and p38 increased remarkably after injection, and peaked at day three [Fig. 7(F)]. Consistent with this, IHC staining showed a significant activation of p-p38 in MIA injected TMJs, especially in the fibrous layer and proliferative layer [Fig. 7(G)].

The *in vitro* model showed that PH-797804, a novel pyridinone-based ATP-competitive inhibitor of p38α, can restrain the MIA-induced increase of CX3CL1. WB showed that the expression of CX3CL1 was remarkably higher in the MIA group, and reduced to normal level in the PH-797804 group. ELISA showed that the soluble form of CX3CL1 gives the same effect, which is significantly high in the MIA group, and low in the PH-797804 group [Fig. 7(H)]. The Transwell experiment showed that the PH-797804 can restrain the enhancement of chemotaxis induced by MIA [Fig. 7I]. This confirmed the regulatory effect of PH-797804 from another perspective, and provided a new target for the treatment of TMJOA.

Discussion

In this study, we demonstrated an increased chemotaxis of OCPs induced by chondrocyte apoptosis in the TMJOA model, which partly explains the spatial relationship between cartilage destruction and bone destruction. In terms of mechanism, we focused on CX3CL1, which is a critical chemokine in the chemotaxis of OCPs. The apoptotic environment enhanced the release of CX3CL1, and was restrained by the application of pan-caspase inhibitor Z-VAD-FMK. This suggests a relationship between apoptosis and chemotaxis in TMJOA chondrocytes. *In vivo* experiments showed that the increase in CX3CL1 within TMJOA could also be seen in the subchondral bone. When the CX3CL1-CX3CR1 axis was blocked, the apoptosis-induced recruitment to OCPs was inhibited and less osteoclast activation occurred. The release of CX3CL1 by apoptotic chondrocytes could be suppressed by the p38α inhibitor PH-797804, indicating that p38 MAPK might also be involved in this process. Taken together, this study proposes that apoptotic chondrocytes recruit OCPs, and thus enhance local osteoclastic activity (Fig. 8). This provides a new prospective target in the treatment of TMJOA, yet due to the limited sample size of this study, the conclusions still need to be verified with further experiments.

Chondrocyte apoptosis plays a critical role in the pathology of OA. Some studies noted that, even though apoptosis is defined as programmed cell death, apoptotic cells also release a variety of signal molecules, attract phagocytes to clean up, and affect the local microenvironment. Cullen *et al.*[37] found that Fas-CD95 promotes the release of a series of cytokines which could attract phagocytic cells. A similar phenomenon was also found in the process of chondrocyte apoptosis in this experiment. In the apoptotic
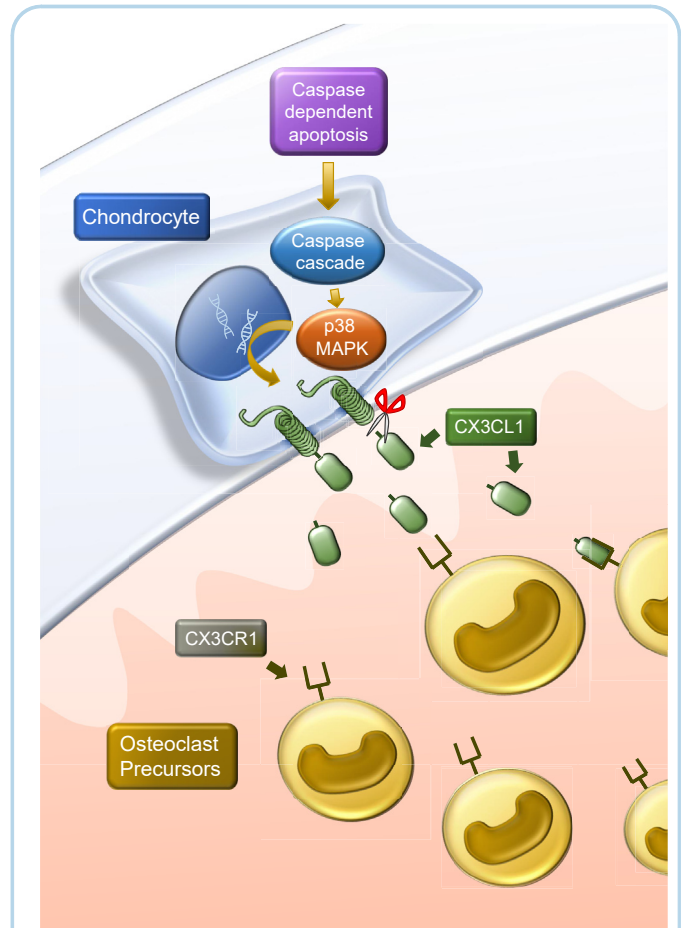

Fig. 8   Osteoarthritis and Cartilage

Diagram of the probable mechanism of OCP-recruitment induced by chondrocyte apoptosis. The upregulation of p38 MAPK increased the release of CX3CL1 in apoptotic chondrocytes, which promotes the chemotaxis of OCPs and ultimately enhanced bone resorption.

environment, the release of CX3CL1, which is a typical molecule with a "find me" signal function, was significantly up-regulated. Interestingly, in the apoptotic environment, the transcription of some other cytokines was also up-regulated, including the chemokines CCL3, CCL22 and MCP-1. This suggests that the impact of the apoptosis process on the local microenvironment may be more

Fig. 7   Osteoarthritis and Cartilage

Activation of p38 MAPK was involved in MIA induced TMJOA model. (A–E) WB was used to determine the change of key molecules of different pathways, including MAPKs, STAT1 and p65, data presented are mean fold change relative to vector control and normalized to β-actin (n = 6). (F) The change in expression of p-p38 at different time-points of the TMJOA model. (G) IHC staining and quantification of p-p38 positive cells in the condylar cartilage. (H) The increase of CX3CL1 induced by MIA was restrained by p38α inhibitor PH-797804. (I) Increased migration of BMMs induced by MIA was restrained by PH-797804, quantified by the number of migrated cells in each view. Data are presented by mean ± SD (n = 6). Two-way ANOVA was used to evaluate the significance between multiple groups in (A, H, I), and *P*-values were calculated by Tukey's test for post-hoc comparisons. One-way ANOVA was used to evaluate the significance between multiple groups in (F, G), and Dunnett test was used to calculate the *P*-value for post-hoc comparisons.

complicated than imagined earlier, and needs to be further explored.

The literature provides no specific answer as to how the apoptotic environment can affect the expression of chemokine CX3CL1. However, the NF-κB, JAK-STAT, and p38 MAPK pathways are clearly involved. NF-κB was found to bind to the promoter of CX3CL1 to regulate its transcription in both respiratory epithelial and bile duct epithelial cells[31,36]. Previous studies showed that the JAK-STAT pathway involved in the regulation of CX3CL1 expression in osteoblasts and in skin/muscle incision and retraction (SMIR)[32,35]. In the model of inflammation-induced CX3CL1 release, the p38 MAPK was significantly activated, and this up-regulation was more significant and sustained than the activation of the NF-κB and other MAPK pathways[34]. O'Sullivan *et al.*[33] verified the regulatory effect of p38 MAPK on the release of CX3CL1, and proposed that this effect may be related to the cleavage and shedding process of CX3CL1. Regarding the regulatory mechanism of CX3CL1 in TMJOA cartilage tissue, there remains a lack of literature verification. In our model, the activation of p38 MAPK was the most significant one, and its inhibitor significantly inhibited the transcription and expression of CX3CL1, indicating the important role it plays in the regulation of CX3CL1 in TMJOA cartilage tissue. It should be noted that the chemotaxis of CX3CL1 is mainly exerted by its soluble form. In follow-up research, we will also pay attention to the regulation of CX3CL1 shedding.

The literature reports that there is a dual chemotaxis-differentiation process from OCPs to mature osteoclasts. OCPs from bone marrow and circulation are attracted to the osteoclast niche, and differentiate into mature osteoclasts after being stimulated[38,39]. The promotion of osteoclast differentiation induced by OA cartilage has been reported[14,15]. Our group has also tested the differentiation-related cytokines, and have consistently reached the same conclusion (Appendix Fig. 2). However, the chemotactic effect of chondrocyte apoptosis on osteoclasts in OA remain unclear. Our study focused on the "chemotaxis" induced by apoptosis, and the role of CX3CL1. That this key factor mediates chemotaxis of OCPs was emphasized for the first time. Considering that osteoclasts have a certain destructive effect on cartilage, this regulatory effect may be mutual. As for which process plays a more important role in the progression of osteoarthritis, and which point is more suitable as a treatment target, we need to further explore.

In conclusion, this study clarifies that apoptotic TMJ condylar chondrocytes have a chemotactic effect on OCPs. We suggest that the regulatory effects of caspases on the chemokine-CX3CL1 associated with the activation of p38 MAPK constitute a new target for the treatment of TMJOA.

Author contributions

Yan Ning Guo, contributed to conception, design, data acquisition, analysis, and interpretation, drafted the manuscript; Sheng Jie Cui, contributed to experimental design, analysis and critically revised the manuscript; Yan Heng Zhou, Ye Hua Gan, Ya Jing Tian, Ning Rui Zhao, Yi Dan Zhang, contributed to the data interpretation, critically revised the manuscript; Xue Dong Wang, contributed to conception, design, and data interpretation, critically revised the manuscript. All authors gave final approval and agree to be accountable for all aspects of the work.

Role of the funding source

Conflict of interest

The authors declare no potential conflicts of interest with respect to the authorship and/or publication of this article.

Acknowledgments

Supplementary data

Supplementary data to this article can be found online at https://doi.org/10.1016/j.joca.2022.04.002.

References

1. Derwich M, Mitus-Kenig M, Pawlowska E. Orally administered NSAIDs-general characteristics and usage in the treatment of temporomandibular joint osteoarthritis-A narrative review. Pharmaceuticals (Basel) 2021;14.
2. de Souza RF, Lovato da Silva CH, Nasser M, Fedorowicz Z, Al-Muharraqi MA. Interventions for the management of temporomandibular joint osteoarthritis. Cochrane Database Syst Rev 2012;2012:Cd007261.
3. Zhang FY, Wang XG, Dong J, Zhang JF, Lü YL. Effect of occlusal splints for the management of patients with myofascial pain: a randomized, controlled, double-blind study. Chinese Med J 2013;126:2270–5.
4. Lei J, Yap AU, Liu MQ, Fu KY. Condylar repair and regeneration in adolescents/young adults with early-stage degenerative temporomandibular joint disease: a randomised controlled study. J Oral Rehabil 2019;46:704–14.
5. Liu Y, Wu JS, Tang YL, Tang YJ, Fei W, Liang XH. Multiple treatment meta-analysis of intra-articular injection for temporomandibular osteoarthritis. J Oral Maxillofac Surg 2020;78:373.e371-373.e318.
6. Datta A, Flynn NR, Barnette DA, Woeltje KF, Miller GP, Swamidass SJ. Machine learning liver-injuring drug interactions with non-steroidal anti-inflammatory drugs (NSAIDs) from a retrospective electronic health record (EHR) cohort. PLoS Comput Biol 2021;17, e1009053.
7. Wang XD, Zhang JN, Gan YH, Zhou YH. Current understanding of pathogenesis and treatment of TMJ osteoarthritis. J Dent Res 2015 May;94(5):666–73.
8. Li L, Shi H, Xie H, Wang L. MRI assessment and histopathologic evaluation of subchondral bone remodeling in temporomandibular joint osteoarthritis: a retrospective study. Oral Surg Oral Med Oral Pathol Oral Radiol 2018;126:355–62.
9. Iijima H, Aoyama T, Tajino J, Ito A, Nagai M, Yamaguchi S, *et al.* Subchondral plate porosity colocalizes with the point of mechanical load during ambulation in a rat knee model of post-traumatic osteoarthritis. Osteoarthritis Cartilage 2016;24: 354–63.

10. Zhou X, Cao H, Yuan Y, Wu W. Biochemical signals mediate the crosstalk between cartilage and bone in osteoarthritis. BioMed Res Int 2020;2020:5720360.

11. Embree M, Ono M, Kilts T, Walker D, Langguth J, Mao J, et al. Role of subchondral bone during early-stage experimental TMJ osteoarthritis. J Dent Res 2011;90:1331–8.

12. Hügle T, Geurts J. What drives osteoarthritis?-synovial versus subchondral bone pathology. Rheumatology 2017;56: 1461–71.

13. Jiao K, Zhang M, Niu L, Yu S, Zhen G, Xian L, et al. Overexpressed TGF-β in subchondral bone leads to mandibular condyle degradation. J Dent Res 2014;93:140–7.

14. Upton AR, Holding CA, Dharmapatni AA, Haynes DR. The expression of RANKL and OPG in the various grades of osteoarthritic cartilage. Rheumatol Int 2012;32:535–40.

15. Kuang B, Zeng Z, Qin Q. Biomechanically stimulated chondrocytes promote osteoclastic bone resorption in the mandibular condyle. Arch Oral Biol 2019;98:248–57.

16. Felson DT. Osteoarthritis as a disease of mechanics. Osteoarthritis Cartilage 2013;21:10–5.

17. Kim HA, Lee YJ, Seong SC, Choe KW, Song YW. Apoptotic chondrocyte death in human osteoarthritis. J Rheumatol 2000;27:455–62.

18. Sharif M, Whitehouse A, Sharman P, Perry M, Adams M. Increased apoptosis in human osteoarthritic cartilage corresponds to reduced cell density and expression of caspase-3. Arthritis Rheum 2004;50:507–15.

19. Zhang M, Zhang J, Lu L, Qiu ZY, Zhang X, Yu SB, et al. Enhancement of chondrocyte autophagy is an early response in the degenerative cartilage of the temporomandibular joint to biomechanical dental stimulation. Apoptosis 2013;18:423–34.

20. Wang XD, Kou XX, He DQ, Zeng MM, Meng Z, Bi RY, et al. Progression of cartilage degradation, bone resorption and pain in rat temporomandibular joint osteoarthritis induced by injection of iodoacetate. PLoS One 2012;7, e45036.

21. Li W, Hu S, Chen X, Shi J. The antioxidant resveratrol protects against chondrocyte apoptosis by regulating the COX-2/NF-κB pathway in created temporomandibular osteoarthritis. BioMed Res Int 2021;2021:9978651.

22. Zhang S, Teo KYW, Chuah SJ, Lai RC, Lim SK, Toh WS. MSC exosomes alleviate temporomandibular joint osteoarthritis by attenuating inflammation and restoring matrix homeostasis. Biomaterials 2019;200:35–47.

23. Wang XD, Kou XX, Meng Z, Bi RY, Liu Y, Zhang JN, et al. Estrogen aggravates iodoacetate-induced temporomandibular joint osteoarthritis. J Dent Res 2013;92:918–24.

24. Nagata S. Apoptosis and clearance of apoptotic cells. Annu Rev Immunol 2018;36:489–517.

25. Truman LA, Ford C, Pasikowska M, Pound JD, Wilkinson SJ, Dumitriu IE, et al. CX3CL1/fractalkine is released from apoptotic lymphocytes to stimulate macrophage chemotaxis. Blood 2008;112(13):5026–36.

26. Sokolowski JD, Chabanon-Hicks CN, Han CZ, Heffron DS, Mandell JW. Fractalkine is a "find-me" signal released by neurons undergoing ethanol-induced apoptosis. Front Cell Neurosci 2014;8:360.

27. Koizumi K, Saitoh Y, Minami T, Takeno N, Tsuneyama K, Miyahara T, et al. Role of CX3CL1/fractalkine in osteoclast differentiation and bone resorption. J Immunol 2009;183:7825–31.

28. Hoshino A, Ueha S, Hanada S, Imai T, Ito M, Yamamoto K, et al. Roles of chemokine receptor CX3CR1 in maintaining murine bone homeostasis through the regulation of both osteoblasts and osteoclasts. J Cell Sci 2013;126:1032–45.

29. Wojdasiewicz P, Poniatowski LA, Kotela A, Deszczyński J, Kotela I, Szukiewicz D. The chemokine CX3CL1 (fractalkine) and its receptor CX3CR1: occurrence and potential role in osteoarthritis. Arch Immunol Ther Exp 2014;62:395–403.

30. Huo LW, Ye YL, Wang GW, Ye YG. Fractalkine (CX3CL1): a biomarker reflecting symptomatic severity in patients with knee osteoarthritis. J Invest Med 2015;63:626–31.

31. Zhou R, Gong AY, Chen D, Miller RE, Eischeid AN, Chen XM. Histone deacetylases and NF-kB signaling coordinate expression of CX3CL1 in epithelial cells in response to microbial challenge by suppressing miR-424 and miR-503. PLoS One 2013;8, e65153.

32. Shen Y, Li D, Li B, Xi P, Zhang Y, Jiang Y, et al. Up-regulation of CX3CL1 via STAT3 contributes to SMIR-induced chronic post-surgical pain. Neurochem Res 2018;43:556–65.

33. O'Sullivan SA, Gasparini F, Mir AK, Dev KK. Fractalkine shedding is mediated by p38 and the ADAM10 protease under pro-inflammatory conditions in human astrocytes. J Neuroinflammation 2016;13:189.

34. Jones BA, Riegsecker S, Rahman A, Beamer M, Aboualaiwi W, Khuder SA, et al. Role of ADAM-17, p38 MAPK, cathepsins, and the proteasome pathway in the synthesis and shedding of fractalkine/CX3CL1 in rheumatoid arthritis. Arthritis Rheum 2013;65:2814–25.

35. Isozaki T, Kasama T, Takahashi R, Odai T, Wakabayashi K, Kanemitsu H, et al. Synergistic induction of CX3CL1 by TNF alpha and IFN gamma in osteoblasts from rheumatoid arthritis: involvement of NF-kappa B and STAT-1 signaling pathways. J Inflamm Res 2008;1:19–28.

36. Bhavsar PK, Sukkar MB, Khorasani N, Lee KY, Chung KF. Glucocorticoid suppression of CX3CL1 (fractalkine) by reduced gene promoter recruitment of NF-kappaB. Faseb J 2008;22: 1807–16.

37. Cullen SP, Henry CM, Kearney CJ, Logue SE, Feoktistova M, Tynan GA, et al. Fas/CD95-induced chemokines can serve as "find-me" signals for apoptotic cells. Mol Cell 2013;49:1034–48.

38. Mizoguchi T, Muto A, Udagawa N, Arai A, Yamashita T, Hosoya A, et al. Identification of cell cycle-arrested quiescent osteoclast precursors in vivo. J Cell Biol 2009;184:541–54.

39. Novak S, Roeder E, Kalinowski J, Jastrzebski S, Aguila HL, Lee S-K, et al. Osteoclasts derive predominantly from bone marrow–resident CX3CR1+ precursor cells in homeostasis, whereas circulating CX3CR1+ cells contribute to osteoclast development during fracture repair. J Immunol 2020;204: 868–78.